A 1-dimensional-two-layer transient drift-flux model for hydraulic transport pipelines modelling and experiments of bed layer erosion and density wave amplification

de Hoog, Edwin; van der Voort, Tjalie; Talmon, Arno; van Rhee, Cees

DOI
10.2478/johh-2023-0039

Publication date
2024

Document Version
Final published version

Published in
Journal of Hydrology and Hydromechanics

J. Hydrol. Hydromech., 72, 2024, 1, 64–79
https://doi.org/10.2478/johh-2023-0039

sciendo Journal of Hydrology and Hydromechanics Institute of Hydrology SAS

A 1-dimensional-two-layer transient drift-flux model for hydraulic transport pipelines: modelling and experiments of bed layer erosion and density wave amplification

Edwin de Hoog[1,2*], Tjalie van der Voort[3], Arno Talmon[4,5], Cees van Rhee[6]

[1] Royal IHC, Smitweg 6, 2961 AW Kinderdijk, The Netherlands. E-mail: e.dehoog@royalihc.com
[2] Department of Dredging engineering, Delft University of Technology, Mekelweg 2, 2628CD Delft. E-mail: e.dehoog@tudelft.nl
[3] Royal IHC, Smitweg 6, 2961 AW Kinderdijk, The Netherlands. E-mail: t.vandervoort@royalihc.com
[4] Department of Dredging Engineering, Delft University of Technology, Mekelweg 2, 2628CD Delft. E-mail: a.m.talmon@tudelft.nl
[5] Deltares, Boussinesqweg 1, 2629 HV Delft. E-mail: arno.talmon@deltares.nl
[6] Department of Dredging engineering, Delft University of Technology, Mekelweg 2, 2628CD Delft. E-mail: c.vanrhee@tudelft.nl
[*] Corresponding author.

Abstract: Hydraulic transport pipelines in the dredging, mining and deep sea mining are designed using steady-state methods. However, these methods cannot predict density wave formation. Density waves form a risk for pipeline blockages, therefore there is a need to understand and preferably be able to model the process. The density waves studied in this research are caused by a stationary sediment deposit in the pipeline. This article explores the development of a new transient design model, based on 1-dimensional-two-layer Driftflux CFD. The two layers model the exchange of sediment between the turbulent suspension, and a stationary bed layer, and can therefore model density wave amplification. An empirical erosion-sedimentation closure relationship is applied to model the sediment exchange between the two layers, and is calibrated using experiments. The final model is also validated against a second experiment, specifically for density wave amplification. The experiments and the model show good agreement on the erosion of a stationary bed layer and the growth rate of a density wave and the amplitude of the density wave.

Keywords: Hydraulic transport; Dredging; Deep sea mining; Transients; Flow assurance; Driftflux.

INTRODUCTION

The dredging, mining and deep sea mining industries use hydraulic transport pipelines, powered by large centrifugal pumps, to transport sediments such as sand, rock, clay, manganese nodules and various other minerals. These pipelines are currently designed using steady-state methods. Specifically, the energy added by the centrifugal pump is weighted against the energy lost by the pipeline. This analysis results in a pipeline operating velocity. When the velocity is high, sediment is suspended by turbulence. When the velocity is low, particles form a bed layer in the pipe. The transition is called: the deposit limit velocity. Steady-state design simply aims to design a pipeline with an operating velocity above the deposit limit velocity.

The steady-state design method unfortunately has its limits, since it is based on steady state assumptions. An example of such a steady assumption is that the concentration of sediment entering the pipeline is constant. Another assumption is that the sediment concentration does not change while flowing through the pipeline. However, various field pipelines and laboratory experiments have shown that these assumptions are not always valid (de Hoog et al., 2021). Variations in mixture concentration, either temporal or spatial, can lead to serious flow assurance issues, mainly in the form of self-excited density waves (de Hoog et al., 2021; Matoušek, 1996; Talmon, 1999). Density waves are highly concentrated flows of sediment, that can self-amplify over time and in space. Density waves form an increased risk to safe pipeline operation, increasing the chance of pipeline blockages, failures of the centrifugal pump drive and complicate future automation of deep sea mining pipelines. In general, the longer the pipeline the greater the risk.

Density waves have so far been encountered as two mechanisms. One where the wave grows due to spatial particle velocity differences between pipes of different orientation, i.e. horizontal and vertical. This was encountered in the “Freiberg” experiments (de Hoog et al., 2022) and referred to as “transient accumulation.” The key characteristic of this mechanism is, that these density waves can form despite that the pipeline operates far above the deposit limit velocity. Therefore, these transient waves cannot be predicted or considered when using steady-state design principles. The second mechanism causes the wave to grow by feeding from a stationary sediment bed layer in the pipeline, when the pipeline operates close to the deposit limit velocity. Erosion of the bed is stronger for higher suspension concentrations above the bed, therefore density waves tend to self-amplify once formed. This mechanism is referred to as the “erosion-sedimentation imbalance” (Talmon, 1999). This article focuses on the latter mechanism, the erosion-sedimentation imbalance.

In the case of waves formed by transient accumulation, a new transient 1-dimensional Computational Fluid Dynamics (CFD) Driftflux model was developed to predict density wave amplification by de Hoog et al. (2022). This type of 1D CFD is very powerful, as it allows the simulation of kilometers long pipelines in a matter of minutes on a decent laptop computer. This is currently impractical with the most state-of-the-art 2D or 3D CFD models (Messa et al., 2021), because of long computational times. Unfortunately, a 1D transient model to predict density waves due to the erosion-sedimentation imbalance is currently not available. Since density waves due to the erosion-sedimentation imbalance are still not fully understood nor modelled, a 1D CFD model would be very

valuable to further research the problem, and potentially also a great design tool for pipeline designers.

The aim of this article is to explore the possibility to model density waves due to the erosion-sedimentation imbalance, using 1D CFD. We propose to extended the 1D model by de Hoog et al. (2022) with a second lower layer, to be able to model the erosion and sedimentation process between the suspended particles and the bed layer. The second lower layer models a stationary bed, while the upper layer models the suspended particles. A closure relationship can be used to model the transfer of sediment between the two layers. A potential candidate for this closure relationship can be found in CFD simulations of other dredging processes and morphological models, specifically empirical "erosion-sedimentation" based models (Bisschop, 2018; Talmon, 1999; van Rijn, 1984; van Rhee, 2010). However, such erosion-sedimentation models have never been applied in pipeline flows before.

In this article we will aim to answer the following research question: Can we model density wave amplification using a 1-dimensional-2-layer (1D-2L) CFD model? A sub question is: Is an erosion-sedimentation based closure relationship suitable for modelling the sediment exchange between the stationary bed layer and the suspended flow, within a 1D-2L model?

First, we create a new numerical scheme for a 1D-2L Driftflux model. Secondly, validation experiments are conducted to validate the use of an erosion-sedimentation closure for pipeline flows. And thirdly, experiments to validate the formation of density waves in the new 1D-2L Driftflux model are conducted. These steps are elaborated in the Methods and Results & Discussion sections. But first, the erosion-sedimentation density wave amplification mechanism is explained in the Theory section.

THEORY

So how does the erosion-sedimentation imbalance work? A density wave can grow from a stationary bed layer in the pipeline, by erosion of the bed. This bed layer is formed when the mixture velocity drops below the deposit limit velocity. Once formed, the bed layer erodes faster for increasingly higher mixture concentrations, due to hindered sedimentation (Talmon, 1999). The concept of hindered sedimentation entails that the sedimentation rate of particles is increasingly hindered, and therefore decreases, with increasing mixture concentration (Richardson and Zaki, 1954). As a consequence, at velocities close to the deposit limit velocity, low concentration flows cause sedimentation, while high concentration flows cause erosion. This unintuitive behaviour led to the name: the erosion-sedimentation imbalance (Talmon, 1999). Consequently, a local maximum of the concentration can act as a small perturbation, which locally causes more erosion than in surrounding areas. This small perturbation will grow, flow further down the pipe, erode the bed more, and consequently grow even more. This process keeps repeating as the wave self-amplifies, until the wave is fully developed.

Mathematically, the erosion and sedimentation of a bed layer can be described with an erosion and sedimentation balance (Bisschop, 2018; Talmon, 1999; van Rijn, 1984; van Rhee, 2010):

$$v_{sed} = \frac{\partial y_b}{\partial t} = \frac{S_h - E_h}{\rho_s(1 - n_0 - c_{nb})} \tag{1}$$

In Equation (1), v_{sed} is the sedimentation velocity of the bed interface, y_b the bed height, t time, ρ_s the particle density, n_0 the bed porosity and c_{nb} the near bed concentration. The near bed concentration represents the concentration responsible for the erosion and sedimentation process, defined to be just above the bed layer (more details in the Methods section). S_h is the hindered settling flux, which is the amount of sediment that settles out of suspension and forms a bed. E_h is the hindered erosion flux, which represents the sediment being eroded and transferred to the suspension. When E_h and S_h are equal to each other, the bed height is steady.

Hindered sedimentation is modelled using the well-known and accepted Richardson and Zaki (1954) approach:

$$S_h = \rho_s w_{ts} c_{nb} (1 - c_{nb})^n \tag{2}$$

In Equations (2) w_{ts} is the terminal settling velocity of a particle, n is the hindered settling exponent and c_{nb} is the near bed concentration. The exponent n can be modeled using Garside et al. (1977).

Unfortunately, hindered erosion is not as well researched as hindered sedimentation. Research by Winterwerp at al. (1992) and van Rhee and Talmon (2010) found experimental proof for hindered erosion at low bed shear stresses. While during the high shear stress experiments by Bisschop (2018) not much focus was put into hindered erosion. Recent work by Keetels et al. (2023) shows that for increasingly higher suspension concentrations erosion is dampened. This is caused by the loss of turbulent kinetic energy at high concentration (>~30%). Under these conditions, turbulence simply cannot pick up more sediment. Keetels et al. (2023) used multi-phase turbulent kinetic equations to derive these conclusions. They tested their theory against a wide range of experimental data, including the data from van Rijn (1984) and Bisschop (2018).

As part of this research it was found that without modelling hindered erosion in the 1D-2L model, density waves grow indefinitely in time. This is because of the $1 - n_0 - c_{nb}$ term in the denominator of Equation (1). This creates an additional numerically based argument, to better model hindered erosion. Specifically, erosion should be damped for concentrations approaching the bed concentration, as stated by Keetels et al. (2023). We propose the following hindered erosion model:

$$E_h = E \cdot \left[1 - \left(\frac{c_{nb}}{c_{max}}\right)^m\right] \tag{3}$$

In which E is the erosion flux without a hindered effect, thus at low near bed concentrations. For $m = 1$ and $c_{max} = 1 - n_0$ the equation equals the hindered erosion model by van Rhee and Talmon (2010). The parameters c_{max} and m require calibration, which will be elaborated in the Results & Discussion section of the article.

Figure 1 shows the results of Equations (1), (2) and (3), and how these can lead to density wave amplification. In this arbitrary example, the bed erodes at a near bed concentration above 20%. This can be seen in Figure 1 when v_{sed} is lower than zero as a function of c_{nb}. As this occurs, the flow switches from a net sedimentation to a net eroding flow. Therefore, a local small concentration perturbation will erode deposits, consequently grow, flow down the pipe, increase the near bed concentration, cause more erosion and cause the wave to grow even more. A constantly repeating cycle of erosion and density wave growth. Concluding, this causes a perturbation to self-amplify.

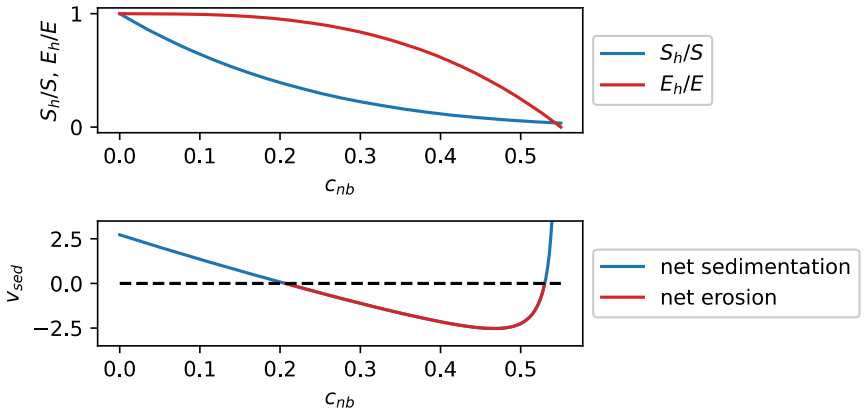

Fig. 1. Top: a visualization of hindered erosion and hindered sedimentation as a function of the near bed concentration. Bottom: an arbitrary example of Equation (1), showing sedimentation for concentrations below 20% and erosion above 20%, using $S = 2.5$, $E = 1$, $m = 3$, $c_{max} = 0.55$.

METHODS

With the erosion-sedimentation imbalance in mind, the following steps need be taken to develop a 1-dimensional-two-layer Driftflux model, which is able to model density wave amplification. Firstly, develop a numerical scheme of a 1D-2L model. The requires implementation of the second layer. Secondly, apply the erosion-sedimentation closure relationship to model the mass exchange between the two layers. Thirdly, experimentally validate the use of an erosion-sedimentation based closure relation in pipeline flow. Lastly, experimentally validate the self-amplification of a density wave. The method sections follow the steps as given above.

Numerical scheme of the 1D-2L Driftflux model

The 1D-2L Driftflux model is based on a self-developed in-house code. The novelty of this model is the two layers and that volume of the cells change in time and space. We use the Finite Volume Method (FVM) to discretize the model, because this method always ensures mass conservation. To further explain the model an illustration of the numerical grid is given in Figure 2.

The 1D-2L model is based on a circular shaped cross-section. In Figure 2 a numerical cell is split into an upper and a lower layer. The upper layer represents the flowing suspended mixture, while the lower layer models the stationary bed layer. The cell size is Δx and the index i denotes the cell number with $i - \frac{1}{2}$ and $i + \frac{1}{2}$ the in- and out- faces of the cell i, respectively. The pipe diameter D and bed layer height y_b are defined on the cell faces and both can change in space. Because only the upper layer flows, the momentum and transport equations will only apply to the upper layer. The volume concentration c, mixture density ρ_m, and momentum $\rho_m \hat{u}_m$ are cell averaged values of the upper flowing layer.

The 1D-2L model requires two types of mixture velocities. Firstly, the mixture velocity $\hat{u}_m$ can be derived from a mass balance of the fluid and solids phases.

$$\hat{u}_m = u_s \frac{\rho_s}{\rho_m} c + u_f \frac{\rho_f}{\rho_m} (1 - c) \tag{4}$$

In Equation (4), c is the cell averaged volumetric concentration, ρ_s and ρ_f are the density of the solids and fluid respectively, and u_s and u_f their respective velocities. This mass flow based mixture velocity is referred to as the Favre averaged mixture velocity is some Driftflux literature, and allows for a convenient way to derive the momentum equation (Ishii and Habiki, 2011).

The second way to define the mixture velocity is based on a volume balance, which is required for the particle transport equation:

$$u_m = u_s c + u_f (1 - c) \tag{5}$$

The full derivation of the momentum and transport equations for this two-layer model, is provided in detail in Appendix A.

The continuity equation for modelling the mass flow on the entire mixture is as follows:

$$\frac{\partial}{\partial t}(\rho_m V) + \sum_{faces} (\rho_m \hat{u}_m \mathrm{A}) = \Gamma_m \tag{6}$$

In which V is the volume of the upper layer cell and A the cross-sectional area of the upper cell face (the area above the bed). The volume of the upper cell V is computed numerically and is a function of D and y_b on both cell faces. This allows for a continuous grid with varying bed heights as well as varying pipe diameters. In Equation (6), the sum over the cell faces represents the in- and out-fluxes F over the cell faces. The mass source term Γ_m is used to exchange mass between the two layers, and is related to the volumetric source term Γ_v as depicted in Figure 2.

To adhere to Newton's second law, the momentum balance is as follows:

$$\begin{aligned} \frac{\partial}{\partial t}(\rho_m \hat{u}_m V) + \sum_{faces} (\rho_m \hat{u}_m \hat{u}_m A) \\ = -\sum_{faces} (pA) - \tau_m O - \tau_b W + \cdots \\ -\rho_m g A \sin(\omega) - \sum_{faces} \Big[A c \rho_s (u_s - \hat{u}_m)^2 \\ + A(1 - c)\rho_f \big(u_f - \hat{u}_m\big)^2 \Big] + A \cdot S_p \end{aligned} \tag{7}$$

In Equation (7), p is the pressure, τ_m the shear stress of the pipe wall, τ_b the shear stress on top of the bed layer, O the surface area of the pipe wall (above the bed), W the surface area

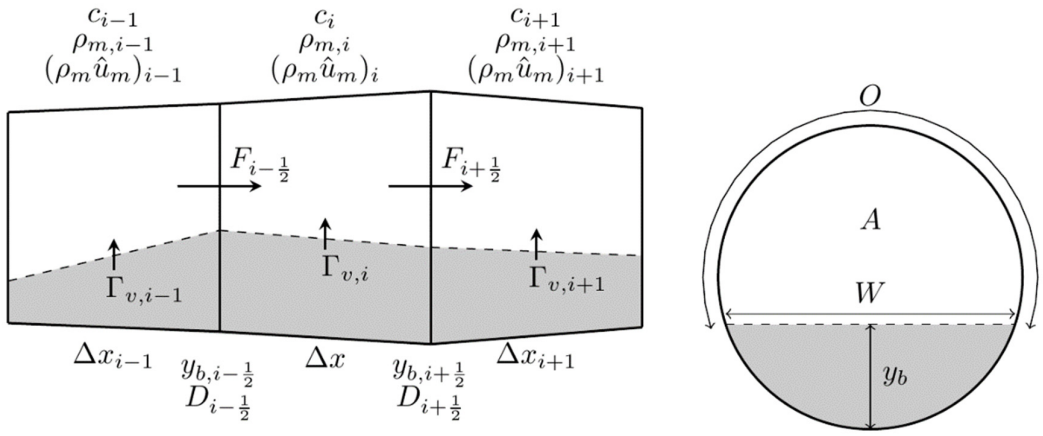

Fig. 2. The grid definition of the 1D-2L Driftflux model. The upper layer represents the flow of sediment and the lower layer the stationary bed. c is the sediment concentration, ρ_m is the mixture density, Δx is the cell size, y_b the bed height, D the pipe diameter, F the numerical fluxes, Γ_v the bed source term, W the bed width and O the pipe wall surface of the cell portion above the bed.

of the bed interface, ω the pipe inclination angle and S_p the centrifugal pump pressure source term.

The particle transport equation, which is required to model the flow of the particles only, is as follows:

$$\frac{\partial}{\partial t}(cV) + \sum_{faces} (u_s c A) = \Gamma_v \tag{8}$$

In Equation (8) u_s is the particle velocity, and Γ_v the erosion-sedimentation volumetric based source term. The particle velocity, required in Equation (5), is modelled as:

$$u_s = u_m + u_{s/m} - \frac{\epsilon}{c}\frac{\partial c}{\partial x} \tag{9}$$

This allows us to model a velocity difference, $u_{s/m}$, between the mixture velocity u_m and the particle velocity u_s. To be able to model axial diffusion due to turbulent dispersion, a diffusion velocity is modeled using the diffusion coefficient ϵ.

The relative particle velocity in the horizontal pipes are estimated with the empirical Sobota and Krill (1992) model:

$$u_{s/m} = -u_m \left[f_t \cdot \left(1 - \frac{c}{0.6}\right)^{2.16} \cdot \left(\frac{u_{crit}}{u_m}\right)^{1.7} \right] \tag{10}$$

With f_t an empirical constant and u_{crit} the critical velocity, which is roughly equal to the deposit limit velocity. f_t is computed as a function of the particle Reynolds number. This particle Reynolds number is based on the particle terminal settling velocity, w_{ts}: $Re_p = \frac{\rho_f w_{ts} d_{50}}{\mu_f}$. This particle Reynolds number should not be confused with other particle Reynolds numbers used in other fields of CFD, which are based on the slip velocity of the particle. f_t is computed as follows:

$$f_t = \begin{cases} 0.1464 \cdot 10^{0.6031 \cdot \log(Re_p)} & \text{if } \log(Re_p) < 1 \\ 0.7858 \cdot \tanh[0.7986 \cdot \log(Re_p)] & \text{if } \log(Re_p) \geq 1 \end{cases} \tag{11}$$

This empirical model is only applicable for mixture velocities above u_{crit}. However, we also need to model the relative particle velocity above the bed layer, thus below u_{crit}. No empirical models are available for this. Therefore, it is proposed to use the same model, but scale u_{crit} with the hydraulic diameter of the reduced flow cross-section above the bed layer, effectively modeling a smaller pipe for the cells above the bed. Since u_{crit} roughly equals the deposit limit velocity, and most empirical models of the deposit limit velocity scale with the square root of the pipe diameter (Visintainer, et al. 2023), we scale u_{crit} accordingly:

$$\frac{u_{crit,h}}{u_{crit}} = \sqrt{\frac{D_h}{D}} \tag{12}$$

In which $u_{crit,h}$ is the critical velocity in case of a bed layer, and D_h the hydraulic diameter of the cross-section above the bed layer. This method allows for a smooth transition when computing $u_{s/m}$ once a bed layer forms, although it is not validated. Fortunately, the effect of $u_{s/m}$ was found not to be very sensitive for predicting density wave amplification, as such this proposed adaption, although not validated, seems a good placeholder until a better closure model is available.

The shear stresses, axial dispersion coefficient ϵ and pump source term S_p are modelled exactly the same way as with the 1D Driftflux model covered by de Hoog et al. (2022). The relative particle velocity $u_{s/m}$ in vertical sections of the grid is modeled differently. Specifically, the relative particle velocity in vertical pipes is based on the hindered settling velocity principle (Richardson and Zaki, 1954), which has been shown to work well in vertical pipes (van Wijk, 2016). Since these aspects are not the focus of this article, we kindly refer you to de Hoog et al. (2022) for these details. Rather, this research's main focus is on the two-layer structure and mass exchange between the two layers.

Modeling erosion and sedimentation of the bed layer

To model the sediment exchange between the two layers, the erosion-sedimentation balance is used (Equation (1)). This choice was made for the following reasons:

1. The original erosion-sedimentation imbalance (Talmon, 1999) was derived using this method. As such, directly numerical modelling this is a good way to further verify the erosion-sedimentation imbalance mechanism.

2. The availability of high bed shear stress erosion data from the research of Bisschop (2018). High bed shear stresses result in a shear layer above the bed, several particle diameters thick, which is different from single particle erosion (Bisschop, 2018). This erosion mechanism is the main erosion mode in pipe flows, due to the typically high velocities encountered in pipelines (in the order of meters per second).

3. Erosion-sedimentation functions have successfully been applied in numerical models for various applications such as alluvial flows, coastal morphology (Delft3D) and sedimentation of sand in trailing suction hopper dredgers.

In the state-of-the-art 2D and 3D multiphase literature, sediment beds are modelled using rheological models or kinetic theory models. The authors are aware of these developments and discuss these further in the Results & Discussion section.

The general formulation of the mass exchange terms in the CFD model need to be explained in more detail. To this end Γ_m is used in Equation (6) and Γ_v in Equation (8). These two source terms both represent the exchange of solids between the bed and the suspension, but have different units. Specifically, Γ_m is in mass flow rates, while Γ_v is in unit volume flow rates. The two are related as follows:

$$\Gamma_m = \Gamma_v \cdot \left[\rho_s - \rho_f \left(1 - \frac{1}{1 - n_0}\right)\right] \tag{13}$$

So how is Γ_v computed? Imagine how the top of bed layer erodes: Particles are lifted from the bed layer into the suspension. In other words, the concentration of sediment transferred to the suspension equals the change of the bed layer volume V_b multiplied by the concentration of the bed, which is equal to $1 - n_0$:

$$\Gamma_v = \frac{\Delta V_b}{\Delta t} \cdot (1 - n_0) \tag{14}$$

The change of the bed layer volume is computed from the change of the height of the bed layer at the cell faces.

$$\frac{\Delta V_{b,i}}{\Delta t} = f\left(\frac{\Delta y_{b,i-\frac{1}{2}}}{\Delta t}, \frac{\Delta y_{b,i+\frac{1}{2}}}{\Delta t}\right) \tag{15}$$

The bed height change at the faces is computed using Equation (1).

The pickup function to model E in Equation (3) needs to be defined next. The Bisschop (2018) model was chosen for two reasons. Firstly, the dataset on which this model is calibrated is of high velocity erosion. This regime is also applicable for our application, and in general suitable for pipeline flows. Secondly, the model is easy to implement numerically and does not require any iteration like a few other pickup functions do. The Bisschop (2018) model is as follows:

$$E = \frac{h_s \lambda_b (1 - n_0) \rho_s}{4\, T_B} \tag{16}$$

In which h_s is the shear layer thickness, λ_b a coefficient to represent the amount of turbulent bursts eroding the bed layer, n_0 the porosity of the sand bed and T_B the mean bursting period of turbulent sweeps. λ_b and T_B have a physical meaning, but can be varied to calibrate the model. Bisschop (2018) recommends $\lambda_b = 1$ and $1.0 < T_b < 3.0$. Bisschop (2018) states that this model requires iterative computation. Fortunately, an explicit solution was found during this research. For further details on implementation of this pickup function, and the explicit solution, see Appendix B. To compute the erosion flux E, the following geotechnical parameters are required: the angle of internal friction ϕ, the maximum porosity of the bed n_{max}, the minimum porosity n_{min} and the permeability at the maximum porosity k_{max}.

The final piece of the puzzle is how to model the near bed concentration. The near bed concentration is the concentration just above the bed layer that dictates the erosion process, and is required for the Bisschop (2018) erosion model. At low concentration or low velocities, the concentration just above the bed layer is equal to the mean concentration of the suspension (van Rijn, 1984). However, at high concentrations or high velocities a shear layer develops above the bed, therefore the near bed concentration becomes a function of the height above the bed. Bisschop (2018) showed that the erosion process at high flows is governed by turbulent eddies eroding parts of the bed layer. These eddies were approximately 3 cm large. Therefore, Bisschop (2018) defined the near bed concentration to be the concentration 3 cm above the bed layer, in a 28.8 cm high conduit. This is roughly at 10% of the total height of the conduit. However, the experiments and simulations in this research are conducted in a 4 cm pipe, therefore direct application of the 3 cm height as defined by Bisschop (2018) is not viable. How to solve this problem? The largest turbulent eddy in a pipe scales linearly with the pipe diameter, or more specifically with the Stokes number (Keetels et al., 2023). Therefore, the 3 cm erosion zone is scaled linearly with the height of the conduit, 28.8 cm in the case of Bisschop (2018) and 4 cm in the experiments of this research. Using this method, an empirical relationship is derived to relate the near bed concentration to the average concentration of the suspended flow, measured form experiments, which are explained in the next subsection. The resulting empirical relationship between the mean suspended concentration and the near bed concentration can be found in the Results & Discussion section.

Experiments to validate the erosion-sedimentation balance in pipe flow

A dedicated experiment was designed to study the implementation of the erosion-sedimentation balance in pipe flow. These experiments are also used to determine an empirical relationship for the near bed concentration as a function of the average concentration of the suspension. A vertically oriented 40 mm diameter pipe circuit was built. This circuit contained a 2 meter long horizontal section, with a vertical inlet and a vertical outlet. An Electrical Resistance Tomograph (ERT) was placed 1.5 meter along this section. This ERT measured the sediment concentration distribution over the cross-section of the pipe over time with a sample rate of 64 Hz. At the inlet and outlet Conductance Concentration Meters (CCM) were placed vertically. The 2-meter measuring section was prepared with a sand bed. A mixing loop, in front of the 2-meter section, was used to prepare a suspended mixture with a desired concentration, by measuring the weight of the sand and knowing the volume of the mixing loop. An Electro-Magnetic Flowmeter (EMF) was placed in front of the mixing loop to measure the mean pipeline velocity. The centrifugal pump was placed before the EMF, at the very start of the flow loop. Figure 3 shows a schematic overview of the experimental apparatus.

The data required to validate the erosion model is the bed height over time, the concentration above the bed layer and the mean pipeline velocity. More data was measured, like pressure losses in the pipes, inlet concentrations, outlet concentrations, however this data is not used as part of this article, and therefore this data is reserved for future publications. At initiation of an

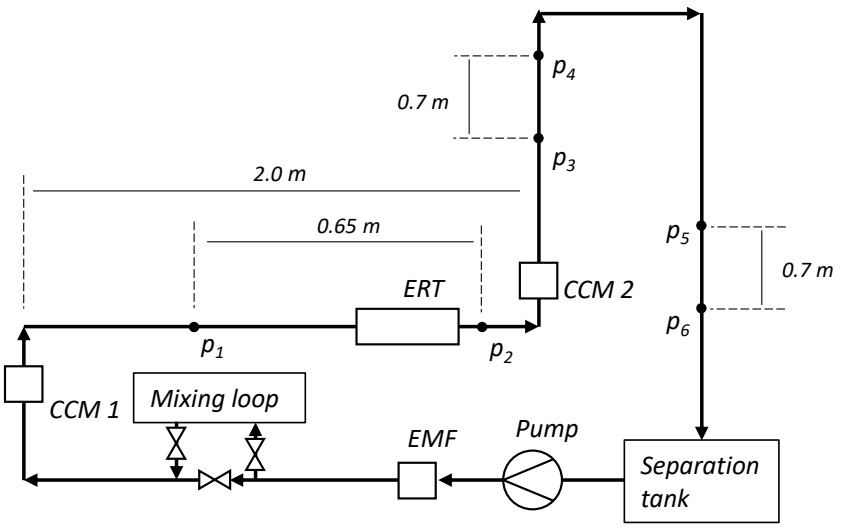

Fig. 3. A schematic front view of the bed erosion experimental setup. ERT = Electrical Resistance Tomograph, CCM = Conductance Concentratoin Meter, EMF = ElectroMagnetic Flowmeter.

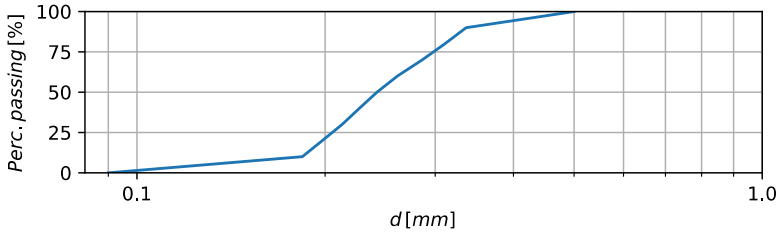

Fig. 4. The particle size distribution of the Zilverzand used for all experiments in this research.

experiment, the main pump was turned on, the mixing loop was connected to the main loop and the prepared mixture was sent past the sand bed. At the end of the loop the sand was separated using a settling tank. The water was sent back into the loop to recirculate.

In total 20 experiments were conducted using five sand types at four different concentrations in the mixing loop, specifically 5, 10, 20 and 30%. The sand types ranged in size from 242 µm to 2 mm. Only the 242 µm sand showed erosion without sliding bed behavior (Zilverzand: $d_{10} = 184$ µm, $d_{50} = 242$ µm, $d_{90} = 336$ µm, see Figure 4 for the particle size distribution). On the contrary, the bed layer of the larger sand types started sliding before being fully dissolved by erosion. The sliding bed mechanism forms different density waves, and is therefore outside of the scope of this research. As such, for validation we have four experiments with 242 µm sand, at mixing loop concentrations of 5, 10, 20 and 30%.

A method is needed to determine the bed height from the ERT tomograms. Figure 5 shows a tomogram of a stationary bed without flow and the pipe filled halfway with a flat sand bed.

Notice that at the side of the tomogram the correct bed concentration is measured, between 50–55%. However, in the middle of the tomogram the concentration is not between 50–55% as it should be. Also notice that the sharp bed interface is not well represented in the tomogram. These two issues are caused by the interpolation algorithm used to construct the tomogram from the raw sensor data, which is provided by the ERT manufacturer and tends to smear out sharp gradients. Because of the non-sharp interface in the tomogram, the actual height of the bed is located somewhere in the smeared out region. This causes an error when computing a bed height from a 1D vertical concentration profile from the tomogram (computed by horizontal integration). To correct for this error, we define that the bed interface is at a concentration of 42%, in the vertical concentration profile. This value was determined through visual observation of a half full pipe, and then interpolation of the tomogram with the method described above. Sharp gradients, like a bed interface, are not present in the suspended parts of the profiles, therefore no correction is applied in these parts of the tomogram.

The near bed concentration is also measured from the concentration tomogram. As explained earlier in the Methods section, the near bed concentration is the concentration of the suspensions 4 mm above the bed layer, which is 10% of the pipe diameter. The near bed concentration is computed by interpolating the vertical concentration profile above the bed. The results of the experiments are presented in the Results & Discussion section.

Experiments to validate erosion-sedimentation based density wave amplification

Another experimental flow loop was built specifically to study density wave amplification, see Figure 6. The loop was built to be as long as possible, in total 45.5 m long at an internal diameter of 42 mm. To measure the density wave development two vertical U-loops were constructed, to measure the delivered concentration c_{vd} (Clift and Clift, 1981; Visintainer et al., 2023), spaced 15.6 m apart. The delivered concentration c_{vd} is defined as the ratio of the solids flow rate over the mixture flow rate.

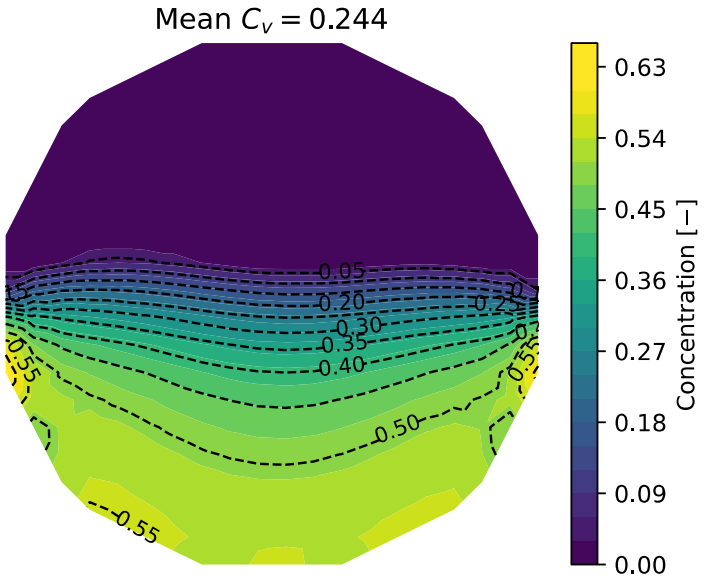

Fig. 5. ERT tomogram of a stationary sharp flat bed interface, without flow over the top. The pipe was filled just below halfway. Notice that at the edges the correct concentration is measured, but the middle of the tomogram does not measure a bed concentration of 50–55%. This is an interpolation error.

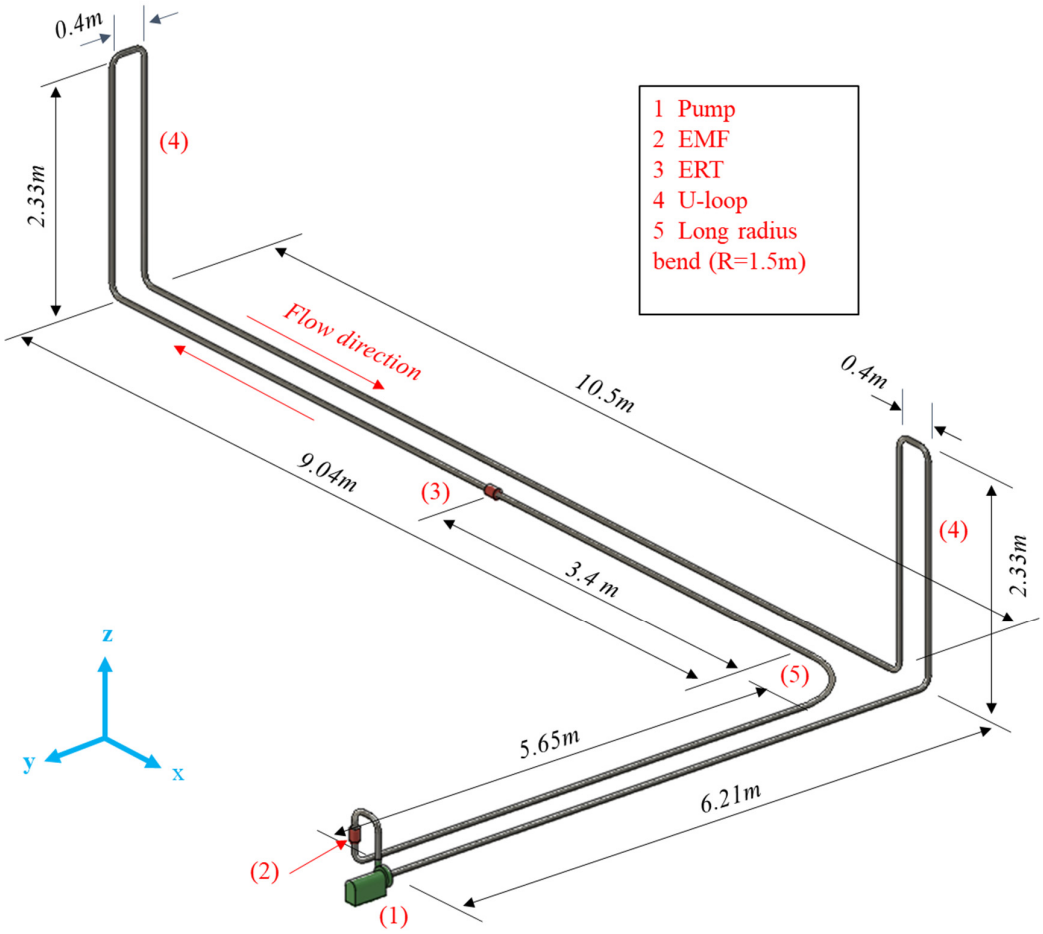

Fig. 6. A 3-dimensional schematic overview of the density wave flow loop. EMF = Electro Magnetic Flowmeter, ERT = Electrical Resistance Tomograph.

The two U-loops were intended to measure the development and growth of a wave between the two loops, this however was an attempt in vain. Figure 7 only displays the signal of the first U-loop downstream of the pump, since displaying both U-loops in one figure clutters the figure too much, and the two measurements are nearly identical. An Electro Magnetic Flowmeter (EMF) was used to measure the velocity of the mixture.

Theoretically, the U-loops affect density wave growth negatively, since these vertical parts do not contribute to density wave development, because no bed layer can form here. To check whether this was a problem, a few test was repeated without U-loops. Fortunately, no change in wave development behaviour could be detected, thus we concluded that the U-loops do not interfere significantly. Furthermore, the dispersive effect of the bends was kept to a minimum by limiting the use of bends only at the U-loops and at the centrifugal pump, and by building a special 1.5-meter long radius bend to complete the circuit. An ERT was also included, but unfortunately the data could not be used, since the ERT could not record data longer then the passing of a density wave. Experiments were conducted with the same Zilverzand as the erosion experiments. Three experiments were conducted with this sand type, at a mean pipeline volumetric concentrations of 10, 15 and 18%. An experiment was conducted in three stages: First, the experiment started at velocities at least twice the deposit limit velocity to disperse any waves. The second step was to slowly lower the pump revolutions until a bed layer formed. The third step was to keep the pump revolutions stable to allow density waves to grow over time. See Figure 7 for an example of the time traces of the pump revolutions, mixture velocity and delivered concentration of one of the experiments. The results of the other experiments, are shown in the Results & Discussion section.

RESULTS & DISCUSSION

In the Methods section the 1D-2L model framework was provided, and the experiments to validate the model explained. So how does the model perform against the experiments?

First the measurements of the near bed concentration are analysed, and an empirical model is derived be able to compute the near bed concentration from the mean concentration of the suspension. The results can be seen in Figure 8, together with the data measured by Bisschop (2018) in the 28.8 cm conduit. The following power-law correlation can be derived from the data:

$$c_{nb} = \min(\, 0.564 \cdot c^{0.252}, c) \tag{17}$$

This equation was fitted through the data in Figure 8, using a non-linear least squares method. The near bed concentration is bounded, to never be below the mean concentration c, since this is physically impossible. Do be aware of the spread in the data visible in Figure 8, caused by the concentration measurement, which will naturally affect the accuracy of the estimation of c_{nb} using Equation (17).

A small side note on Figure 8: An error was found in the data processing algorithms to determine the near-bed concentration by Bisschop (2018). The error was corrected, shown in Figure 8, which has not yet been published elsewhere. The original data can be found back in Bisschop (2018; Figure 8.12a).

Next we review the performance of the erosion-sedimentation closure by comparing the model to the experiments. The 1D-2L model was applied in a flow driven mode. This means that the volumetric flow rate is used as input for the model, and the pressure field follows as a results from the momentum equation. Additionally, the initial bed height from the experiment is an initial condition for the model. The near bed concentration was calculated from the mean concentration above the bed as measured by the ERT, using Equation (17). Ideally, the erosion model should be in agreement with all four experiments using the same model settings. Figures 9, 10, 11 and 12 show the results of the erosion experiments against the model, conducted at mixing loop concentrations of 5, 10, 20 and 30% respectively. The Bisschop (2018) model was slightly adjusted, by using $\lambda_b = 0.7$ instead of the default value of $\lambda_b = 1.0$ (see Appendix B for more details). Other geotechnical parameters used in the simulation are: $n_0 = 0.44$, $n_{max} = 0.47$, $n_{min} = 0.36$, $k_{max} = 4.74\text{E}-04\ m/s$, $\phi = 34°$. These were measured by Bisschop (2018). For the hindered erosion model $m = 3.0$ and $c_{max} = 0.55$ were used for all four simulations. The exponent m was found to have a strong effect on the high concentration experiments. By comparing the time required to erode the bed, we can see that by using the above mentioned settings, all four experiments can be simulated to satisfactory agreement. Two trends were noticed during calibration of the erosion model.

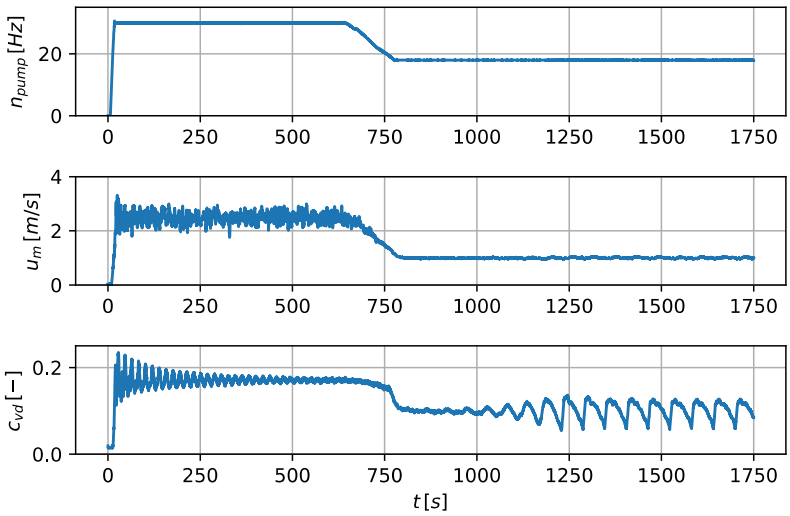

Fig. 7. An example data set of the density wave experiments, using Zilverzand at a concentration of 18%. Top: the pump revolutions. Middle: the mixture velocity. Bottom: the delivered concentration.

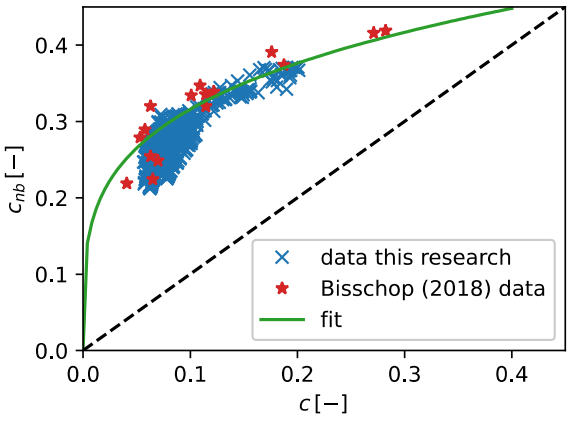

Fig. 8. The near bed concentration c_{nb} as a function of the mean suspended concentration above the bed c. Measured values are from Bisschop (2018) and of the erosion experiments in this research.

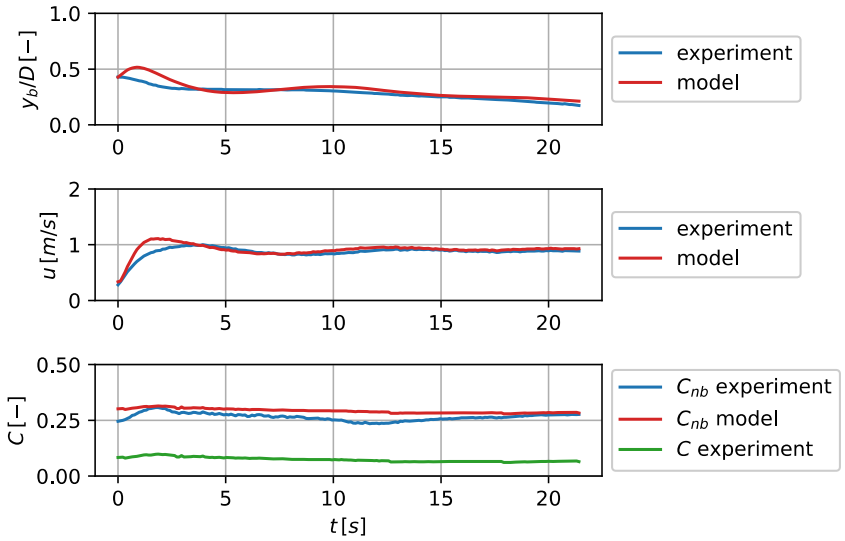

Fig. 9. Model output against experiments, mixing loop concentration is 5%. Top: the bed height, middle: the velocity above the bed, bottom: the near bed concentration.

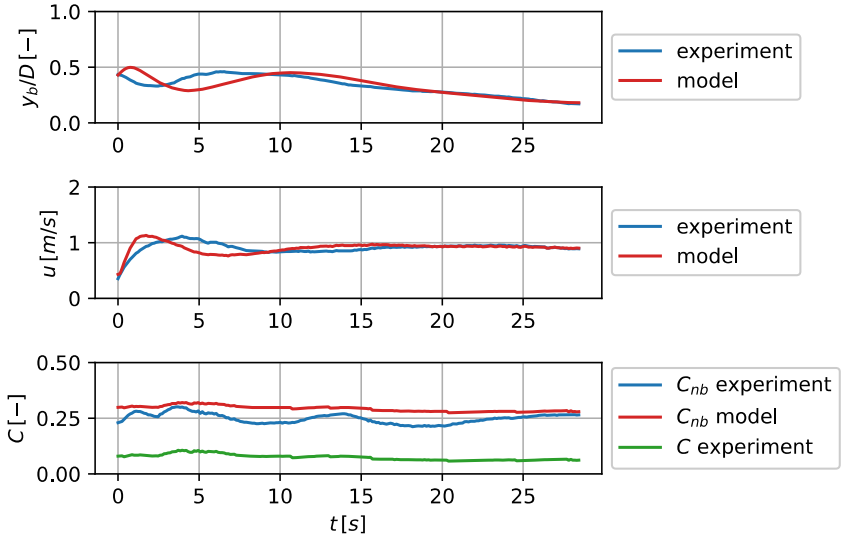

Fig. 10. Model output against experiments, mixing loop concentration is 10%. Top: the bed height, middle: the mean velocity above the bed, bottom: the near bed concentration.

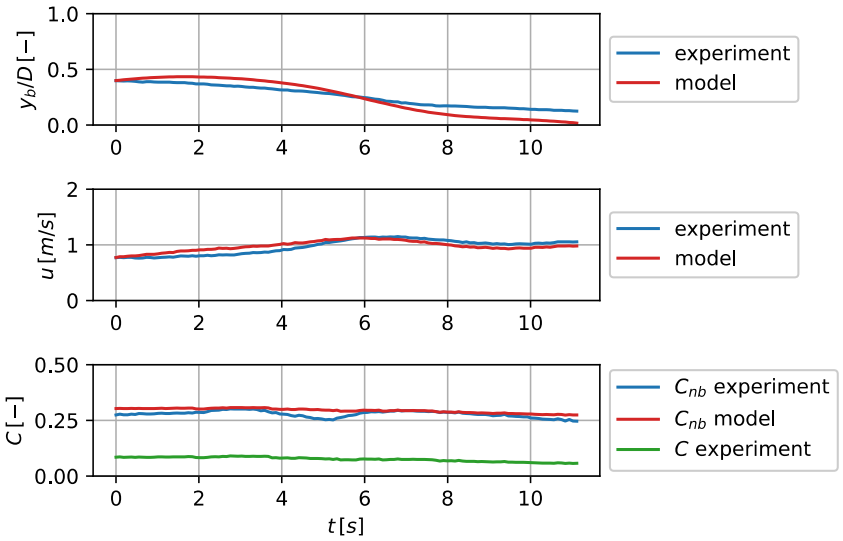

Fig. 11. Model output against experiments, mixing loop concentration is 20%. Top: the bed height, middle: the velocity above the bed, bottom: the near bed concentration.

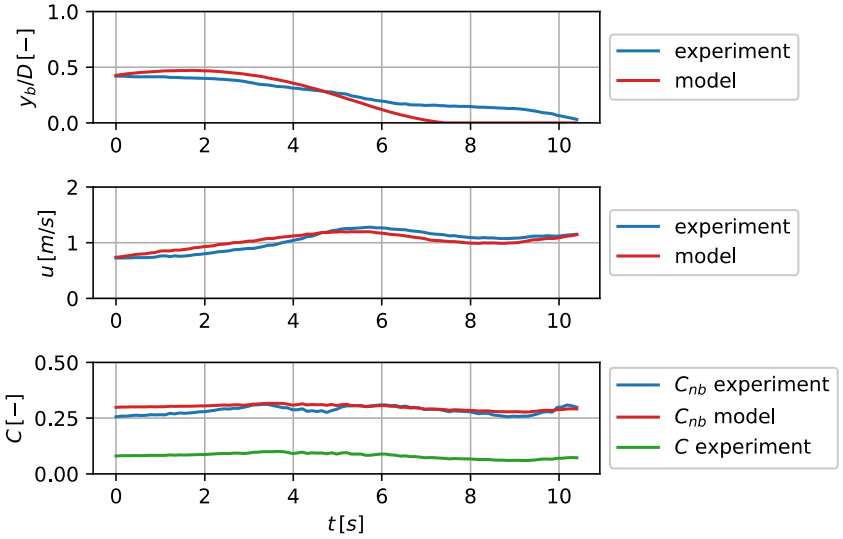

Fig. 12. Model output against experiments, mixing loop concentration is 30%. Top: the bed height, middle: the mean velocity above the bed, bottom: the near bed concentration.

Firstly, for high concentrations the results are sensitive for the hindered erosion model settings, m and c_{max}. Secondly, the calibration was also sensitive to adjustment in the erosion model, λ_b, for all concentrations. A disagreement can be noticed in Figure 12. Figure 12 shows that the experiment lasts 10.5 seconds, while the model predicts a fully eroded bed after 7.5 seconds. In other words, the erosion is slightly overestimated at high concentrations. This behaviour can be altered by recalibrating the hindered erosion model. Calibrating m and c_{max} to better match Figure 12 was attempted, however this made the calibration of Figures 10 and 11 worse, therefore m and c_{max} were left unaltered. In the introduction we asked ourselves: Is an erosion-sedimentation based closure relationship suitable for modelling the sediment exchange between the stationary bed layer and the suspended flow? We can conclude that the answer is yes, after proper calibration of the coefficients. However, if a future goal is to have a generic 1D-2L model for a large range of pipe diameters and sand type, more experimental data is required for validation and calibration, more on this at the end of the discussion section.

Now the ability of the 1D-2L model to simulate density wave amplification is analysed, using the calibrated erosion model. The simulations of the density wave experiments are given in Figures 13, 14 and 15. The full flow loop was meshed including U-loops, with a mesh resolution of 0.1 meter and a time step of 0.01 seconds. From experience using the 1D model, it is generally recommended to have several hundred grid cells to represent a single density wave. These simulations typically produced two waves in the flow loop, as such we used ~250 cells to capture one wave. The time step is based on attaining a Courant grid number lower than 0.1. A good agreement is reached if the amplification rate and density wave amplitude are similar in the experiment and the simulation. The solver once again is used in a flow driven mode. The simulation starts at high velocity similar to the experiment. In the experiment several minutes are used to

allow the wave to dampen, this is not simulated. What is simulated, is a very small initial wave with a length equal to the loop. This was to provide a perturbation for the waves to grow from, and was also present in the experiments. Thereafter, the velocity is lowered over a period of several minutes until a bed layer formed in the simulations. The formation of the bed coincides with a rapid drop of the delivered concentration measured by the vertical U-loops. The experiments showed that the effect of the waves on the mixture velocity was small, and can be considered as constant, see Figure 7. Therefore, in the simulations, once a bed layer formed, the simulated velocity is kept constant as well. The magnitude of the simulated velocity was chosen to attain a bed height similar as measured in the experiments.

We chose to aim for a similar bed height in the simulation compared to the experiment, because the bed height determines the amount of sediment available to create a wave, therefore this influences the final wave amplitude. This was experienced in the experiment, and also during calibration of parameters m and c_{max} for the simulations. The consequence of this choice is however, that the mixture velocity cannot be perfectly matched, since there is some discrepancy between the erosion model and the experiment at high concentrations as seen in Figure 12. The cause of this discrepancy was already addressed three paragraphs earlier in this article. This discrepancy directly results in the mixture velocity mismatch. It was also attempted to do it the other way around, aim for a similar mixture velocity, however then only a very thin bed, or no bed at all formed in the simulations, since the 1D-2L model slightly underestimates the deposit limit velocity. For future research, it is recommended to improve the hindered erosion model (likely not by simply adjusting the coefficients) to be able to predict the deposition limit velocity more accurately.

While calibrating the hindered erosion model, it was found that m influences mainly the amplification rate of the wave, and c_{max} the final wave amplitude. Experiment 1 and 2 (Figures 14 and 15, respectively) could be simulated well with the same settings of the hindered erosion model, using $m = 3$ and $c_{max} = 0.55$. However, with these settings simulation 3 showed waves with a 33% lower amplitude than the experiments, shown in Figure 15. Figure 16 again shows experiment 3, but now using $c_{max} = 0.56$. This gives a better match with the experiment in terms of wave amplitude, and also gives a demonstration of how changing c_{max} affects the wave amplitude.

Table 1 provided an overview of typical values defining the simulation and the experiments. Summarized, the following similarities can be seen between the simulations and the experiments:

1. Wave amplitude: Simulation and experiment are within a 10% deviation for simulation 1 and 2. Simulation number 3 was slightly off when using the same model settings, a 33% deviation.
2. The mean mixture velocity: the simulation predicts a slightly lower mean velocity, and within a 25% deviation.
3. The average delivered concentration of the wave: Simulation and experiment are within a 10% deviation.

One very obvious difference between the simulations and the experiment is the wavelength. In the experiment the wavelength always equals the length of the flow loop, which has also been observed in other density wave experiments (de Hoog et al., 2021; Talmon et al., 2007). These simulations however, usually end up generating two waves. Sometimes the secondary wave was small enough to be absorbed by the main wave, resulting in a single wave, but this did not always occur. Talmon (1999) stated that the relative strength between dispersive forces (ϵ in Equation (9)) and amplifying forces, determines the wave length. However, changing ϵ in the model did not affect the wave length, but only the amplitude. Another hypothesis was that the U-loops affect the wave length. The idea was that the U-loops split the circuit into two sections, since in the U-loops no bed layer can form, because the pipes are vertical. Consequently, the U-loops do not contribute to the density wave amplification process. As such, the hypothesis was that the two U-loops slip the flow loop into two sections, causing two waves to be initialized once a bed layer forms. However, removing the U-loops from the simulation domain made no noticeable difference to the simulations, and still two waves formed in most simulations. Concluding, at this moment it is unclear why the simulations tend to generate two waves in the loop.

In the introduction we asked ourselves the following main research question: Can we model density wave formation using a 1-dimensional-2-layer CFD model? The answer is yes, after calibration of the coefficient. Some remarks: the method chosen in this research is very empirical. The calibration coefficients are λ_b , m , c_{max} and the coefficients related to the c_{nb} model (Equation (17)). The Bisschop (2018) erosion model has a physical foundation, and is calibrated for sand sizes up to 562 μm, therefore has potential to scale well beyond the current use in this article. The hindered erosion and c_{nb} models however are purely empirical, and therefore if any user desires to apply the 1D-2L model in its current state, the user is limited to a pipe of 42 mm and sand of 242 µm.

To transform the 1D-2L model from a research model to a generic design model using the current closures, a large amount of validation data is needed of various pipe diameters and sediment types. This is not advised, rather a better development path would be to use physical based closure from literature. For example, the near bed concentration model can be improved by estimating the concentration distribution above the bed using Schmidt-Rouse type turbulent diffusion models (Matoušek et al., 2014). The fact that a c_{nb} model is required, is linked to the choice of using the Bisschop (2018) erosion model, which is currently the state-of-the-art in the category of physical-empirical erosion models. Using a different closure to model erosion would eliminate the need for the c_{nb} model. An alternative for the Bisschop (2018) could be found in the state-of-the-art 3D multiphase CFD literature, where stationary sediment beds are modelled using rheological models (Chauchat et al., 2017; Goeree, 2018) or using kinetic theory (Berzi and

Table 1. The parameters defining the density wave simulations and experiments.

Simulation/ experiment	Initial concentration [–]		Mean wave concentration [–]		Wave max-min [–]		Mean pipe velocity [m/s]		Relative bed height [–]		m [–]	c_{max} [–]
	Sim	Exp	Sim	Exp	Sim	Exp	Sim	Exp	Sim	Exp		
1	0.10	0.10	0.058	0.054	0.052	0.048	0.82	1.1	0.05	0.06	3.0	0.55
2	0.15	0.15	0.086	0.084	0.071	0.068	0.82	1.0	0.15	0.14	3.0	0.55
3	0.18	0.18	0.12	0.13	0.060	0.090	0.81	1.1	0.12	0.11	3.0	0.55
3*	0.18	0.18	0.12	0.13	0.093	0.090	0.80	1.1	0.14	0.11	3.0	0.56

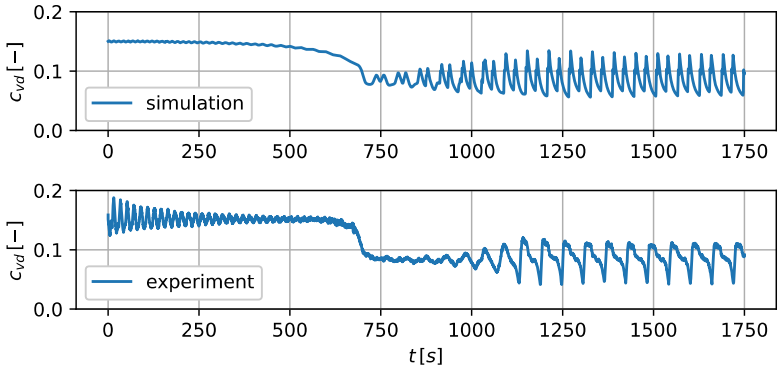

Fig. 13. Results of simulation 1 (top) and experiment 1 (bottom), with an initial concentration of 10%.

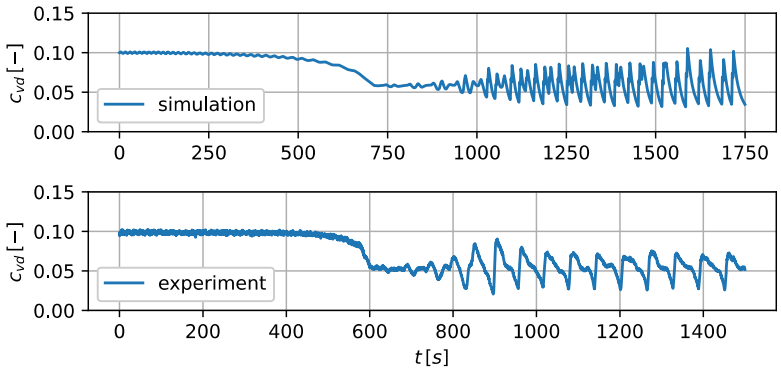

Fig. 14. Results of simulation 2 (top) and experiment 2 (bottom), with an initial concentration of 15%.

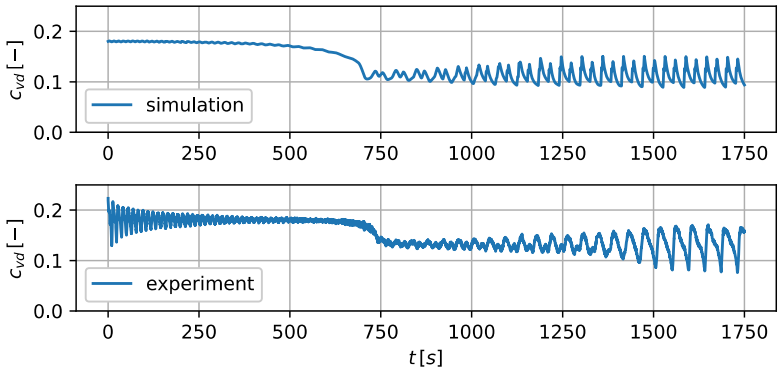

Fig. 15. Results of simulation 3 (top) and experiment 3 (bottom), with an initial concentration of 18%.

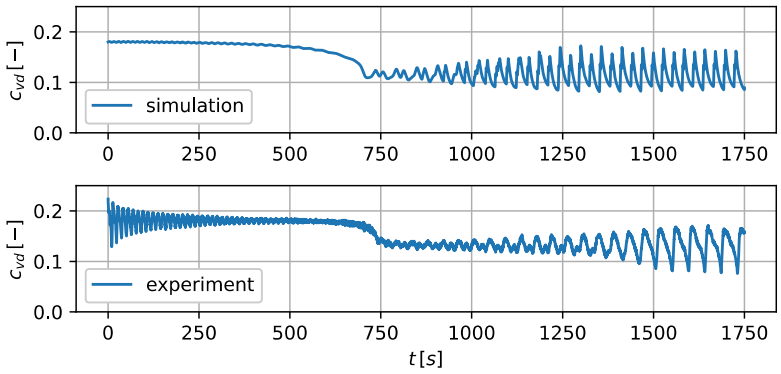

Fig. 16. Results of simulation 3 (top) and experiment 3 (bottom), with an initial concentration of 18%. Using $c_{max} = 0.56$.

Jenkins, 2011). Rheological or kinetic theory based models incorporate more physics, therefore these are better for scaling. This further reduced the demand for experimental data. As such, it is worth investigating the use of a 1D variation of either a rheological or a kinetic theory based model, inspired on the state-of-the-art in 3D multiphase CFD literature.

Up to this point the 1D-2L model was only used in a flow driven mode, as opposed to the pressure driven mode. In the pressure driven mode a driving pressure is applied in one of the cells (representative of a centrifugal pump), and consequently the velocity field follows from the momentum equation. The fully pressure driven mode has been verified and observed to work well, but still requires detailed validation. To verify the pressure driven mode, and therefore the full momentum equation, the energy losses of the bed layer and the mixture should match the experiments. This can be achieved with well-developed physical-empirical models from literature (Visintainer et al., 2023). A pump can be modelled to drive the system to overcome these losses. This will yield a mixture velocity similar to the experiment, and therefore also lead to density waves. This approach also allows for the ability to simulate pipeline blockages, when the density waves grows to large and forms a plug. A similar approach was used with the 1D Driftflux model in de Hoog et al. (2022). Validation of the pressure driven mode of the 1D-2L model will be conducted in the future.

Using the pressure driven mode also enables the possibility to study the role a centrifugal pump booster stations might have in triggering density waves, as hypothesized by de Hoog et al. (2021). The idea is that once a strong wave is formed, and flows through a pump booster station further down the pipe, which is not designed with enough power to handle the wave, causes a pipeline wide drop in mixture velocity. This decrease in velocity can trigger a new wave, if the mixture velocity drops below the deposit limit velocity. This effect is repeated if the new wave flows through the booster pump once more. Resulting in an unstable pipeline, constantly initiating new waves. Even through the 1D-2L model is only validated for a single particle size and pipe diameter, this wave-pump interaction can already be studied. Furthermore, the physics behind wave-pump interaction is easily scaled and translated to larger pipeline diameters, by using pump affinity laws.

CONCLUSIONS

The main aim of this research was to study the possibly to model density wave amplification, caused by the erosion-sedimentation imbalance, using a 1D-2L numerical model. This model helps us understand the density wave phenomenon better, and opens the way towards using 1D transient modelling in pipeline design, to expand on the traditional steady state design methods. The 1D Driftflux model of de Hoog et al. (2022) was used as a starting point, and extended with a changing cell volume in time and space, allowing implementation of a second stationary bed layer. This 1D-2L model uses erosion-sedimentation equations to model the mass transfer between a stationary bed and the suspension, calibrated using custom erosion experiments. Finally, the 1D-2L model was calibrated against density wave experiments and shown to be able to model density wave amplification. The fact that the 1D-2L model can predict density wave amplification, further confirms the erosion-sedimentation imbalance mechanism. This result confirms that the erosion-sedimentation imbalance effect, is a driving mechanism behind density wave formation, in the presence of a stationary bed layer. Even though the model is only 1D, it shows to be able to simulate complex physical processes like bed erosion and density waves, which is a promising result on the path of further developing these type of models and using 1D modeling in daily pipeline design.

Acknowledgements. Thanks are in order to Andre van den Bosch and Ed Stok for the construction of the erosion experiments. We thank Oscar van der Ven for his work done in the density wave experiments and Yarno Ketting of the support in creating this flow loop. A very special thanks need to go to Cees van Rhee, full professor in Dredging Engineering. As a pioneer he introduced us to the exciting topic of deep-sea mining. Cees unexpectedly passed away at the age of 64. We will remember him as a dear colleague and inspiring mentor. This research was funded by Royal IHC and TKI Maritiem.

REFERENCES

Berzi, D., Jenkins, J.T., 2011. Surface flows of inelastic spheres. Physics of Fluids, 23, 1, 013303.

Bisschop, F., 2018. Erosion of Sand at High flow velocities. PhD Thesis. Delft University of Technology, Delft, the Netherlands.

Chauchat, J., Cheng, Z., Nagel, T., Bonamy, C., Hsu, T.J., 2017. SedFoam-2.0: A 3-D two-phase flow numerical model for sediment transport. Geoscientific Model Development, 10, 12, 4367–4392.

Clift, R., Clift, D.H., 1981. Continuous measurement of the density of flowing slurries. International Journal of Multiphase Flow, 7, 5, 555–561.

Garside, J., Al-Dibouni, M., 1977. Velocity-voidage relationships for fluidization and sedimentation in solid-liquid systems. Industrial & Engineering Chemistry Process Design and Development, 16, 2, 206–214.

Goeree, J.C., 2018. Drift-flux modeling of hyper-concentrated solid-liquid flows in dredging applications. PhD Thesis. Delft University of Technology.

de Hoog, E., Talmon, A.M., van Rhee, C., 2021. Unstable transients affecting flow assurance during hydraulic transportation of granular two-phase slurries. Journal of Hydraulic Engineering, 147, 9, 04021029.

de Hoog, E., van Wijk, J.M., Talmon, A.M., van Rhee, C., 2022. Predicting density wave amplification of settling slurries using a 1D Driftux model. Powder Technology, 400, 3, 117252.

Hirsch, C., 2007. Numerical Computation of Internal & External Flows. 2nd Ed. Elsevier, Oxford, UK.

Ishii, M., Hibiki, T., 2011. Thermo-Fluid Dynamics of Two-Phase Flows. 2nd Ed. Springer, US.

Keetels, G.H., Chauchat, J., Breugem, W.P., 2023. Role of turbulent kinetic energy modulation by particle–fluid interaction in sediment pick-up. Journal of Fluid Mechanics, 955, 1, A37 1–29.

Matoušek, V., 1996. Unsteady solids flow in a long slurry pipeline with pumps in series - process of material aggregation. Journal of Hydrology and Hydromechanics, 44, 6, 396–409.

Matoušek, V., Krupička, J., Pěník, V., 2014. Distribution of medium-to-coarse glass beads in slurry pipe flow: Evaluation of measured concentration profiles. Particulate Science and Technology, 32, 2, 186–196.

Messa, G.V., Yang, Q., Adedeji, O.E., Chára, Z., Duarte, C.A.R., Matoušek, V., Rasteiro, M.G., Sanders, R.S., Silva, R.C., de Souza, F.J., 2021. Computational fluid dynamics modelling of liquid–solid slurry flows in pipelines: State-of-the-art and future perspectives. Processes, 9, 9, 1566.

Richardson, J.F., Zaki, W.N., 1954. Sedimentation and

fluidisation: Part 1. Transactions Institution of Chemical Engineers, 32, 35.
Sobota, J., Kril, S.I., 1992. Liquid and solids velocity during mixture flow. In: Proceedings 10th Int. Kolloquium Massenguttransport durch Rohrleitungen. Univ. GH-Paderborn, 20-22 May 1992, Meschede, Germany.
Talmon, A.M., 1999. Mathematical analysis of the amplification of density variations in long-distance sand transport pipelines. In: Proceedings 14th Conference on Hydrotransport, Maastricht, the Netherlands, pp. 3–20.
Talmon, A. M., Aanen, L., Bakker-Vos, R., 2007. Laboratory tests on self-excitation of concentration fluctuations in slurry pipelines. Journal of Hydraulic Research, 45, 5, 653–660.
van Rhee, C., 2010. Sediment entrainment at high flow velocity. Journal of Hydraulic Engineering, 136, 9, 572–582.
van Rhee, C., Talmon, A.M., 2010. Sedimentation and erosion of sediment at high solids concentration. In: Proceedings 18th Conference on Hydrotransport, Bedforshire, UK, pp. 211–222.
van Rijn, L.C., 1984. Sediment pick-up function. Journal of Hydraulic Engineering, 110, 10, 1494–1502.
Visintainer, R., Matoušek, V., Pullum, L., Sellgren, A., 2023. Slurry Transport Using Centrifugal Pumps. 4th Ed. Springer Cham, Switzerland.
van Wijk, J.M., 2016. Vertical hydraulic transport for deep sea mining. PhD Thesis. Delft University of Technology. Delft, the Netherlands.
Winterwerp, J.C., Bakker, W.T., Mastberg, D.R., van Rossum, H., 1992. Hyperconcentrated sand-water mixture flows over a flat bed. Journal of Hydraulic Engineering, 118, 11, 1508–1525.

Received 13 June 2023
Accepted 22 August 2023

APPENDIX A
General Finite Volume Method formulation

According to (Hirsch 2007) the general formulation of the Finite Volume Method in integral form, for a scalar quantity U, is:

$$\frac{\partial}{\partial t}\int_V U\, dV + \oint_S \vec{F}\cdot d\vec{S} = \int_V q\, dV \tag{A.1}$$

where V is the volume of a numerical cell, S the surface of a cell, $\vec{F}$ the numerical flux and q a source term. This equation can be rewritten in a discrete form by expressing volume integrals as volume averaged values, and surface integrals as a sum of numerical fluxes of cell boundaries:

$$\frac{\partial}{\partial t}(U\,V) + \sum_{faces} \vec{F}\cdot\Delta\vec{S} = qV \tag{A.2}$$

The numerical flux $\vec{F}$ equals the product of the scalar value U and velocity $\vec{u}$:

$$\vec{F} = U\,\vec{u} \tag{A.3}$$

For the numerical grid defined by Figure 2, S equals the area of the cell boundary above the bed, A. The source term is rewritten to a volumetric source term per unit time:

$$\Gamma_v = q\,V \tag{A.4}$$

Therefore, the final general formulation of the FVM for 1D grid in Figure 2 becomes:

$$\frac{\partial}{\partial t}(U\,V) + \sum_{faces}(F\,A) = \Gamma_v \tag{A.5}$$

Transport equation

To derive the transport equation of the solids phase, and using the 1D grid defined in Figure 2 and $U = c$, $F = u_s$.

$$\frac{\partial}{\partial t}(cV) + \sum_{faces}(u_s c A) = \Gamma_v \tag{A.6}$$

This can be rewritten in differential form by applying $V = \Delta x A$:

$$\frac{\partial}{\partial t}(cA) + \frac{\partial}{\partial x}(u_s c A) = \Gamma_v \tag{A.7}$$

Momentum equation

To derive the momentum equation of the mixture the sum over the momentum equations of the phases is applied. Therefore, first the momentum equation of a phase is derived. Equation (A.1) is applied in vector form, with $\vec{U} = c_k\rho_k\vec{u}_k$, with c_k, ρ_k and u_k being the respective phase volumetric concentration, density and velocity:

$$\frac{\partial}{\partial t}\int_V c_k\rho_k\vec{u}_k\, dV + \oint_S c_k\rho_k\vec{u}_k(\vec{u}_k\cdot d\vec{S}) = \int_V c_k\vec{f}_k\, dV \tag{A.8}$$

With $\vec{f}_k$ being a force term, which is the sum of internal forces $\vec{f}_{k,i}$ and external forces $\vec{f}_{k,e}$. According to Hirsch (2007), internal forces $\vec{f}_{k,i}$ and external forces $\vec{f}_{k,e}$ can be applied as momentum source terms. Internal forces are:

$$\vec{f}_{k,i} = \boldsymbol{\sigma}\cdot\vec{n} \tag{A.9}$$

With $\vec{n}$ the unit vector and $\boldsymbol{\sigma}$ the total internal stress tensor:

$$\boldsymbol{\sigma} = -p_k \boldsymbol{I} + \boldsymbol{\tau} \tag{A.10}$$

In the above $\boldsymbol{I}$ is the unit tensor, p_k the pressure of a phase and $\boldsymbol{\tau}$ internal viscous stresses, which represent internal friction forces between fluid layers. Since the model is 1D, internal viscous stresses cannot be modelled in this way, rather momentum source terms are applied (see Equation (A.21)). Pressure is only resolved in axial direction. Therefore, the source term for internal forces simply reduces to:

$$f_{k,i} = -p_k \tag{A.11}$$

Hirsch (2007) states that internal forces act as surface sources, therefore are integrated over the cell surfaces. The momentum equation of a phase now becomes:

$$\begin{aligned} \frac{\partial}{\partial t}\int_V c_k \rho_k \vec{u}_k \, dV + \oint_S c_k \rho_k \vec{u}_k (\vec{u}_k \cdot d\vec{S}) \\ = -\oint_S c_k p \cdot d\vec{S} + \int_V \vec{f}_{k,e} \, dV \end{aligned} \tag{A.12}$$

For the 1D numerical grid defined by Figure 2, S equals the area of the cell boundary above the bed, A. The 1D momentum equation of a phase becomes:

$$\begin{aligned} \frac{\partial}{\partial t}(c_k \rho_k u_k V) + \sum_{faces} (c_k \rho_k u_k u_k A) \\ = -\sum_{faces} (c_k p_k A) + c_k F_{k,e} \end{aligned} \tag{A.13}$$

With $F_{k,e}$ being the total integrated phase external force acting on a volume V, and the "faces" being the numerical cell faces. The mixture density ρ_m, by summation of all phases k, is defined as:

$$\rho_m = \sum_{k=0}^{N} c_k \rho_k \tag{A.14}$$

The Favre averaged mixture velocity is $\hat{u}_m$ defined as (Ishii and Hibiki, 2011):

$$\hat{u}_m = \frac{1}{\rho_m} \sum_{k=0}^{N} c_k \rho_k u_k \tag{A.15}$$

The drift velocity $u_{k/m}$ is defined as the velocity difference between the phase and the mixture velocity:

$$u_{k/m} = u_k - \hat{u}_m \tag{A.16}$$

Summation of the drift velocity over all fraction must equal zero (Ishii and Hibiki, 2011):

$$\sum_{k=0}^{N} c_k \rho_k u_{k/m} = 0 \tag{A.17}$$

Finally, the mixture momentum equation is attained by summing Equation (A.13) over all k phases:

$$\begin{aligned} \frac{\partial}{\partial t}\sum_{k=0}^{N}(c_k \rho_k u_k V) + \sum_{faces}\left[\sum_{k=0}^{N}(c_k \rho_k u_k u_k A)\right] \\ = -\sum_{faces}\left[\sum_{k=0}^{N}(c_k p_k A)\right] \\ + \sum_{k=0}^{N} c_k F_{k,e} \end{aligned} \tag{A.18}$$

Substitution of Equations (A.14), (A.15), (A.16) by applying (A.17), into (A.18), leads to the mixture momentum equation:

$$\begin{aligned} \frac{\partial}{\partial t}(\rho_m \hat{u}_m V) + \sum_{faces}(\rho_m \hat{u}_m \hat{u}_m A) = -\sum_{faces}(pA) \\ + \cdots \\ - \sum_{faces}\left[\sum_{k=0}^{N} A c_k \rho_k u_{k/m} u_{k/m}\right] \\ + F_e \end{aligned} \tag{A.19}$$

In which p is the pressure of the mixture and F_e the external forces on the entire mixture. The equation is slightly rewritten. Specifically, the water phase ($k = 0$) is replaced by subscript f, the solids phase ($k = 1$) with subscript s:

$$\begin{aligned} \frac{\partial}{\partial t}(\rho_m \hat{u}_m V) + \sum_{faces}(\rho_m \hat{u}_m \hat{u}_m A) = -\sum_{faces}(pA) \\ + \cdots \\ - \sum_{faces}\left[Ac\rho_s(u_s - \hat{u}_m)^2 + A(1-c)\rho_f(u_f - \hat{u}_m)^2\right] \\ + F_e \end{aligned} \tag{A.20}$$

In which F_e are external frictional forces over the entire mixture and p the pressure over the mixture. The external forces are:

$$F_e = -F_m - F_b - F_s + F_p \tag{A.21}$$

In which F_m are frictional forces of the mixture against the pipe wall, F_b frictional forces of the mixture flow over a bed layer, F_s hydrostatic forces and F_p are driving forces caused by the pressure of the pump.

$$F_m = \tau_m O \tag{A.22}$$

$$F_b = \tau_b W \tag{A.23}$$

$$F_s = \rho_m g A \sin(\omega) \tag{A.24}$$

$$F_p = A\, S_p \tag{A.25}$$

The final momentum equation becomes:

$$\begin{aligned} \frac{\partial}{\partial t}(\rho_m \hat{u}_m V) + \sum_{faces}(\rho_m \hat{u}_m \hat{u}_m A) \\ = -\sum_{faces}(pA) - \tau_m O - \tau_b W \\ + \cdots \\ -\rho_m g A \sin(\omega) - \sum_{faces}\left[Ac\rho_s(u_s - \hat{u}_m)^2\right. \\ \left. + A(1-c)\rho_f(u_f - \hat{u}_m)^2\right] + A\, S_p \end{aligned} \tag{A.26}$$

APPENDIX B – BISSCHOP (2018) PICKUP FUNCTION EXPLICIT SOLUTION

The erosion model by Bisschop (2018) is a physical-analytical model, based on turbulent sweeps eroding parts of the bed layer. The pick function of Bisschop (2018) is as follows:

$$E = \frac{h_s \lambda_b (1 - n_0) \rho_s}{4 T_B} \tag{B.1}$$

With h_s the shear layer thickness, ρ_s the particle density, n_0 the bed porosity, λ_b a coefficient for the amount to turbulent bursts eroding the bed layer and T_B the mean bursting period of a turbulent sweep. The shear layer thickness is estimated with:

$$h_s = (p' - \sigma_a) \cdot \frac{\tan\left(\frac{\pi}{4} + \frac{\phi}{2}\right)}{N_\gamma g (\rho_s - \rho_f + i \cdot \rho_f)} \tag{B.2}$$

With p' the normal pressure on the sand bed caused by turbulent bursts, σ_a the resisting pressure of a sand wedge in the bed to be removed by turbulent bursts, ϕ the sand internal friction angle, N_γ a soil strength related constant, ρ_b the in-situ density of the sand bed and i the hydraulic gradient caused by inward flow of water normal to the bed layer, due to soil dilatation. The normal pressure p' is calculated as:

$$p' = \frac{1}{2} \rho_f \hat{w}^2 \tag{B.3}$$

With $\hat{w}$ the mean vertical velocity of the turbulent bursts, which is a function of the mixture velocity above the bed u_b.

$$\hat{w} = 1.0 \cdot u_b \tag{B.4}$$

The sand bed resistance vertical pressure σ_a equals:

$$\sigma_a = \frac{h_s u_b}{2 T_B} \rho_s (1 - n_0) \tag{B.5}$$

The hydraulic gradient of the bed water inflow i is calculated as:

$$i = \frac{h_s}{T_B \cdot k_{max}} \cdot \frac{n_{max} - n_0}{1 - n_{max}} \tag{B.6}$$

In the equation above n_{max} is the maximum porosity the soil can have, and k_{max} the permeability at n_{max}. N_γ is computed as:

$$N_\gamma = \frac{1}{2}\left[\left(\frac{1 + \sin\phi}{1 - \sin\phi}\right)^{5/2} - \left(\frac{1 + \sin\phi}{1 - \sin\phi}\right)^{1/2}\right] \tag{B.7}$$

Bisschop (2018) states this model needs to be solved iteratively as both σ_a and i are a function of h_s. Fortunately, by substitution of Equations (B.5) and (B.6) into Equation (B.2), a second order polynomial equation can be derived with the following analytical solution:

$$h_s = \frac{-C_1 + (C_1^2 + C_2)^{0.5}}{C_3} \tag{B.8}$$

$$C_1 = \frac{\rho_s}{2}(1 - n_0)\frac{u_b}{T_B} \cdot \tan\left(\frac{\pi}{4} + \frac{\phi}{2}\right) \tag{B.9}$$

$$C_2 = \frac{4}{T_B k_{max}}\left(\frac{n_{max} - n_0}{1 - n_{max}}\right) \cdot N_\gamma \cdot g \cdot \rho_f \cdot p' \cdot \tan\left(\frac{\pi}{4} + \frac{\phi}{2}\right) \tag{B.10}$$

$$C_3 = \frac{2}{T_B k_{max}}\left(\frac{n_{max} - n_0}{1 - n_{max}}\right) \cdot N_\gamma \cdot g \cdot \rho_f \tag{B.11}$$